Optimization of Electrospun Polylactide-Based Ultrathin Fibers for Osteoconductive Bone Scaffolds

Sergio Torres-Giner,[1] Jose V. Gimeno-Alcañiz,[2] Maria J. Ocio,[1,3] Jose M. Lagaron[1]

[1]*Novel Materials and Nanotechnology Group, IATA-CSIC, Avda. Agustín Escardino 7, 46980, Burjassot, Spain*
[2]*Cell culture Laboratory, IATA-CSIC, Avda. Agustín Escardino 7, 46980, Burjassot, Spain*
[3]*Departmento Medicina Preventiva, Faculty of Pharmacy, University of Valencia, 46100 Burjassot, Spain*

Received 6 July 2010; accepted 19 January 2011
DOI 10.1002/app.34208
Published online 19 May 2011 in Wiley Online Library (wileyonlinelibrary.com).

ABSTRACT: Bone tissue interfacial scaffolds, which encourage cell growth, are critical determinants for clinical success after implant surgery. Over the years, a number of resorbable configurations have emerged for bone cell support and growth, but only a few have demonstrated clinical efficacy. Polymer coatings produced by electrospinning are regarded as very promising bone interfaces because of the ultrathin-scaled dimensions of its physical structure. In this study, the morphology, composition, thermal properties, and cell growth viability of a number of polylactide-based systems containing different binary and ternary formulations of this biomaterial with collagen and commercial hydroxyapatite nanoparticles were characterized. The best performance in terms of biocompatibility was obtained for the tricomponent system in which the submicron fibers were further subjected to uniaxial orientation process during formation. The *in vitro* proliferation of the cells, which harbored on these ultrathin-structured mats, was examined by means of a metabolic activity indicator and ensured by means of scanning electron microscopy, and cell anchorage was checked by fluorescent optical microscopy. Finally, the optimum tricomponent material was successfully sterilized for the first time by gamma radiation without noticeable losses in cell-seeding capacity.
 J Appl Polym Sci 122: 914–925, 2011

Key words: polylactide; electrospinning; bioactive fibers; bone interfaces

INTRODUCTION

Polylactide or polylactic acid (PLA), probably, the most attractive and useful biodegradable synthetic aliphatic polyester, has been extensively studied for a wide number of applications.[1] A large number of PLA-based materials are being currently carried out in biomedical applications, for instance, in bone substitution, either as resorbable implants (can be slowly broken down into nontoxic metabolites by bio-organisms)[2] or as drug-delivery vehicles.[3] However, the ranges of application of PLA as biomedical scaffold can be somewhat restricted because of the limited cell viability, poor hydrophilicity as well as high rigidity and crystallinity.[4] To overcome these limitations, various blends of PLA with other materials have been pursued, such as their collagen blends,[5] the biohybrid blends with hydroxyapatite nanoparticles (nHA),[6] or even both.[7] In any bone-regenerative applications, the addition of these two biomaterials usually results in an improvement in bioactivity, because they can mimic the main solid natural bone-forming components.[8]

The current commercial process of producing PLA and other polyester-based materials for biomedical applications is generally a braiding of melt-spun filaments, which are either used as suture materials or woven into mats to serve as tissue dressings.[9] A major limitation of such commercially available scaffolds is their relatively large fiber sizes (10–12 μm), which are due to the limitations of traditional extrusion.[10] Most recent deliberations consider that proper *in vivo* phenotype cannot be achieved when cells are presented with fibers that possess diameters equal to the cell size or, in many cases, an order of magnitude greater.[11] In addition, fibers with nanoscale morphologies may provide improved transport of nutrients, metabolites, and soluble factors of the seeded cells, which are essential to regenerate the desired tissue structures.[12] Observational evidence for this conclusion comes from a particular consideration of the native extracellular matrices (ECM) of various tissues, in which fibers are quite frequently one or more orders of magnitude smaller than the cells themselves, and these appear to have a highly intricate 3-D relationship with their ECM structures.[13] This represents a unique challenge for the fabrication of tissue-engineering scaffolds.

Correspondence to: J. M. Lagaron (lagaron@iata.csic.es).
Contract grant sponsor: MEC; contract grant numbers: MAT2009-14533-C02-01, MAT2006-10261-C03.
Contract grant sponsors: Nanobiomatters Ltd. (Spain) and the IP of the EU FP6, NEWBONE.

In this context, the electrospinning technology has emerged as one of the most effective methods to fabricate artificial scaffolds that are composed of a large network of interconnected submicron fibers.[14] Electrospun coatings can approximate the nanostructural morphology of the ordinary bone surface by assessing appropriate levels and sizes of porosity to allow cell migration, sufficient surface area, and a variety of surface chemistries to encourage cell proliferation and differentiation, and adjustable degradation rate to match natural regeneration.[15] Electrospinning is then able to generate osteoconductivity, because, by definition, an osteoconductive surface is one that promotes bone growth on its surface or down into pores, channels, or pipes.[16] To date, electrospinning has been used for the fabrication of promising biomedical scaffolds from numerous resorbable biopolymers, in particular, including PLA[17,18] and PLA with collagen.[19] Other studies have reported about the fabrication of electrospun PLA fibers based on bioceramics, such as nanohydroxyapatite (nHA),[20,21] and, more recently, bioactive glass.[22]

Because of the bending instability associated with the spinning technology jet, electrospun fibers are often deposited on the collector surface (a single piece of conductive substrate) as randomly oriented nonwoven mats, which could be unsatisfactory depending on their application.[23] Electrospun fibers, mostly oriented parallel to each other along the edge, can also be prepared by using a mandrel or rotating disk collector, and such intentional alignment can achieve higher levels of cell adhesion and proliferation by mimicking native bones.[24] In particular, the aligned architecture favors the cell–fiber interactions by means of directional growth of the cells along the fiber orientation.[25] The aligned fiber structures also provide for increased control of porosity[26] and improved mechanical integrity,[27] properties desirable in osteoconductive substrates.

Furthermore, it is mandatory in clinically relevant constructs to sterilize all artificial implants if at all possible without inducing chemical changes. Gamma irradiation (γ-irradiation) from a 60Co source is a clean, convenient, and effective method for the sterilization of implant materials, in which an approximate radiation dosage of 2.5 Mrad (25 kGy) is required to achieve complete sterilization.[28] In particular, the effect of γ-irradiation on the biological properties of biomedical implants has been studied in detail principally on polymer-based materials.[29] Several studies on the effect of radiation on collagen-based biomaterials such as with γ-irradiation[28] or ultraviolet light[30] have clearly indicated chain scission resulting in protein fractions of lower molecular weight. However, very little research is known on the effect of γ-irradiation on any type of PLA, and there is no report on PLA electrospun coatings.

In this original study, we present a novel scaffold based on electrospun coatings of PLA-based submicrofibers with the inclusion of low amounts of a bioactive inorganic nanostructured elements. The chosen growth-inductive components to enhance the cellular behavior were collagen and nHA, which are constitutive elements of the ordinary bone. For the first time, a promising tissue-engineered aligned submicron-construct, based on a tricomponent fibrous system (PLA, collagen, and nHA), was fabricated using electrospinning and then sterilized by γ-irradiation.

EXPERIMENTAL

Materials

The semicrystalline PLA used was a film extrusion grade produced by Natureworks (USA) with a D-isomer content of ~2%. The molecular weight had a number–average molecular weight (M_n) of ~130,000 g/mol, and the weight–average molecular weight (M_w) was ~150,000 g/mol as reported by the manufacturer. Lyophilized collagen, Bornstein and Traub Type I, from calf skin was purchased from Elastin Products Company (USA). Pyrogenesis (Greece) graciously supplied a commercial grade of nanohydroxyapatite, so-called nHA, without further description, which has been specifically developed within an integrated project called NEWBONE of the EU FP6 program. 1,1,1,3,3,3-Hexafluoro-2-propanol (HFP) and fluorescein diacetate (FD) were purchased from Sigma-Aldrich (Spain).

Electrospinning process

Electrospinning was performed by using a plastic syringe containing the polymer solutions on a digitally controlled syringe pump while the needle was oriented in vertical toward the collector. Further details of the basic electrospinning setup can be found elsewhere.[31] Polymer solutions containing 6 wt % of PLA and of blends of PLA/collagen 85/15 (wt/wt) and PLA/collagen/nHA 75/15/10 (wt/wt) were prepared in HFP solvent at room temperature under magnetic stirring. The governing parameters were fixed at 12 kV of power voltage, 14 cm of tip-to-collector distance, and 0.20 mL/h of volumetric flow rate. Collagen nanofiber mats were prepared by electrospinning from a 5 wt % collagen solution in aqueous HFP 85 wt % with the governing parameters fixed at 11 kV of power voltage, 12 cm of tip-to-collector distance, and 0.25 mL/h of volumetric flow rate.[30] A mandrel connected to ground, disposed in horizontal at 14 cm from the tip, was used to collect the aligned fibers. The mandrel-rotating speed was fixed at

3000 rpm. Environmental conditions were maintained stable at 24°C and 60%RH by having the equipment enclosed in a specific chamber with temperature and humidity control.

Sterilization

The electrospun PLA/collagen/nHA fibers were irradiated with γ-ray from a 60Co source at room temperature at a dose of 2.5 mrad by Aragogamma S.A. (Spain). The fibers were received as fully sterilized according to manufacture specifications.

Morphology

The as-spun fibers were examined using scanning electron microscopy (SEM; *S*-4100) from Hitachi (Japan) at 8.0 kV, after having been sputtered with a gold–palladium mixture in vacuum. Fiber diameters were measured by means of the Adobe Photoshop 7.0 software from the SEM micrographs by manual size determination of ~ 300 fibers from the SEM micrographs in their original magnification. Transmission electron microscopy (TEM) was performed using a JEOL 1010 (Canada) equipped with a digital Bioscan (USA) image acquisition system. TEM pictures were taken on fibers directly electrospun onto the TEM observation grids. Cell images were taken using phase-contrast technique with an inverted optical microscope Nikon Eclipse TE2000-S (Japan) coupled to a digital camera (Digital Sight DS-5M-L1). A fluorescent FITC filter of EX 465–495 nm BA 515–555 nm coupled with an optical microscope Nikon Eclipse 90i (Japan) was used to check cell anchorage.

ATR-FTIR

Attenuated total reflection-Fourier transform infrared (ATR-FTIR) spectra were collected at 24°C and 40%RH coupling the ATR accessory GoldenGate of Specac (UK) to a Bruker Tensor 37 FTIR equipment (Germany). The spectra were collected in the materials by averaging 10 scans at 4 cm^{-1} resolution.

Thermal analysis

Differential scanning calorimetry (DSC) of typically 2 mg of the materials was conducted on a Perkin–Elmer DSC 7 thermal analysis system at a scanning speed of 10°C/min. The thermal history applied was a heating scan from 40 to 180°C. Before evaluation, the thermal runs were subtracted analogous runs of an empty pan. The DSC equipment was calibrated using indium as a standard. PLA crystallinity was estimated from the ratio between the heat of fusion of the studied material (corrected for the actual PLA fraction in the blend) and the heat of fusion of an infinity crystal of same material:

$$\%X_c = \frac{\Delta H_f}{\Delta H_f^0} \cdot 100 \quad (1)$$

where ΔH_f is the enthalpy of fusion of the studied specimen and ΔH_f^0 is the enthalpy of fusion of a totally crystalline material. The ΔH_f^0 fed to the equation was 93 J/g for PLA.[32]

Thermal gravimetric analysis (TGA) was measured by using a TG/ATD Setaram 16/18 equipment (France), and the temperature was programmed from ambient to 800°C with a heating rate of 5°C/min in Argon on sample masses of ~ 10 mg.

Cell viability

Osteoblastlike cells of human osteosarcoma MG-63 cell line, obtained from European Collection of Cell Cultures, were cultured in a humidified atmosphere of 5% CO_2 at 37°C, in minimum essential medium Eagle from Sigma-Aldrich (Spain) supplemented with 10% fetal bovine serum, 1% penicillin–streptomycin, 1% L-glutamine 200 m*M*, and 1% amphotericin B solutions (v-%) from Hyclone (USA). About 3×10^4 cells/disc were plated in a 24-well culture plate with 1 mL of medium. Proliferation measurements were based on the cellular metabolic activity using the Alamar Blue™ colorimetric indicator dye from Invitrogen (USA) in a Multiskan spectrophotometer from Thermo (USA). Further details of the cell growth measurements can be found elsewhere.[30]

Cell anchorage

In the fluorescent analysis to check cell anchorage, cells were first stained with FD at a concentration of 15 μ*M* and then incubated at 37°C overnight to complete the labeling process, and finally the dye was discarded by washing several times the cells with phosphate-buffered saline (PBS).

RESULTS AND DISCUSSION

Morphology

The morphology of the electrospun mats made of pure PLA, PLA/collagen (which will be referred in the text from now on as the bicomponent system), PLA/collagen/nHA (as tricomponent system), and sterilized tricomponent system fibers are shown in the SEM micrographs of Figure 1. These images show that all electrospun PLA-based fibers appear to be circular in the cross section and devoid of any beads under the selected electrospinning conditions. The electrospun pure PLA fibers on the collector

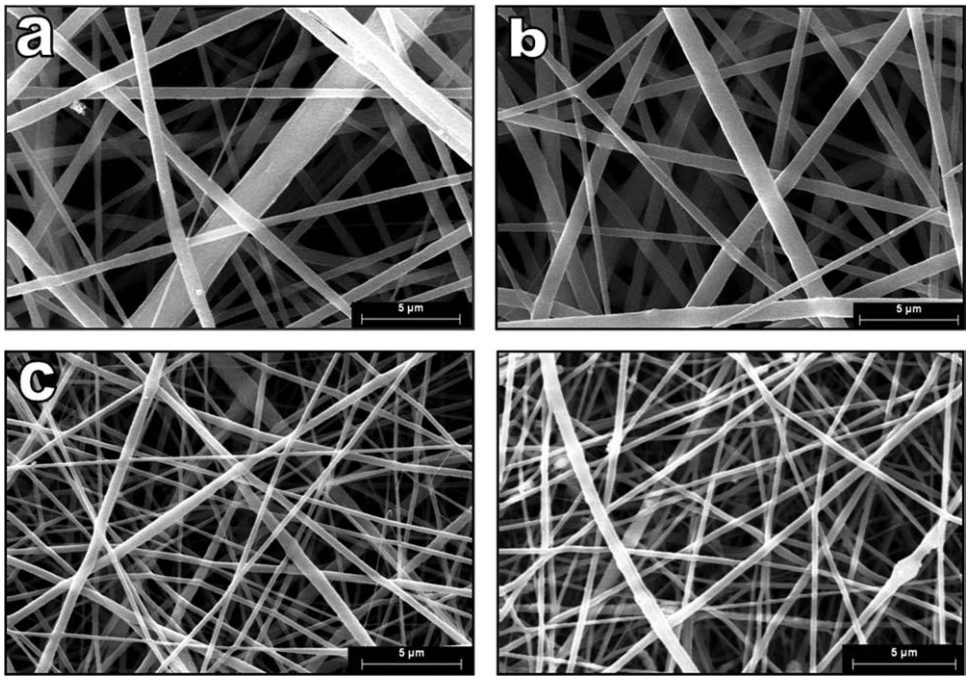

Figure 1 SEM images of the electrospun mats of (a) PLA, (b) bicomponent system, (c) tricomponent system, and (d) sterilized tricomponent system. The scale marker is 5 μm.

formed a randomly oriented nonwoven fabric structure having a bimodal diametric distribution with diameters 1376 ± 211 and 295 ± 140 nm [see Fig. 1(a)]. The bimodal morphology has been previously attributed to the split of the jet resulting in the formation of fibers of different diameters.[31,33–35] It can also be observed, especially in the thicker fibers, that fiber surfaces presented some porous structures. The formation of pores has been already observed for PLA fibers and postulated to be a result of the high volatility of the chosen solvent.[33] Nanoporosity in electrospun polymer fibers can also be produced by a high humid ambient.[36] In Figure 1(b), it can be seen that introduction of collagen to PLA produced a slight reduction in the mean fiber diameter, that is, down to 597 ± 185 nm, and, moreover, the fibers lost most of their bimodal distribution as well as the porous structure. A similar effect on the electrospun morphology has been observed before when mixing two polymers, which are known to produce different electrospun sizes, and so they generally result in intermediate fiber sizes.[35] This is so because it is known that electrospinning of pure collagen protein at similar conditions yields thinner fibers, mainly nanofibers (106 ± 22 nm).[30] Additionally, as Figure 1(c) shows, introducing nHA produced uniformly distributed ultrathin fibers of 362 ± 165 nm cross section size. It is also expected that thinner fibers be generated, because the polymer concentration is reduced. Reducing the concentration is known to lead to smaller fiber diameters ought to a viscosity decrease.[31,35,37] Figure 1(d) also presents the tricomponent mats after sterilization with γ-irradiation in which the fiber morphology is not seen to be different, neither crosslinked nor partially denaturated, as supported by the absence of changes in morphology as previously reported.[30] Finally, Figure 2 presents the diameter distribution for all the studied PLA-based fibers.

Electrospinning can also be used to incorporate structural morphological variations into an engineered material by regulating the orientation of fibrils within the fabricated network. Substantial orientation of the fibers constituting the electrospun mats was obtained by using a rotating drum as collector, which has been considered as a simple and versatile method to generate such unique-aligned topographies.[24–27] Controlling the spatial orientation of electrospun fibers was feasible, and dry aligned roundlike meshes were thus formed as seen in Figure 3. In general, tubular scaffolds are usually needed for most engineered tissues, and the possibility to produce roundlike structures with a certain degree of orientation to favor cell in-growth is of significant relevance.

Dispersion of nHA

Structural studies of naturally occurring apatite crystals in bone have shown that they are intimately related to collagen fibrils[38] and, in particular, have indicated that the mineral phase is well aligned with the fiber direction.[39] These works stated that, presumably, the nanocrystals themselves tend to

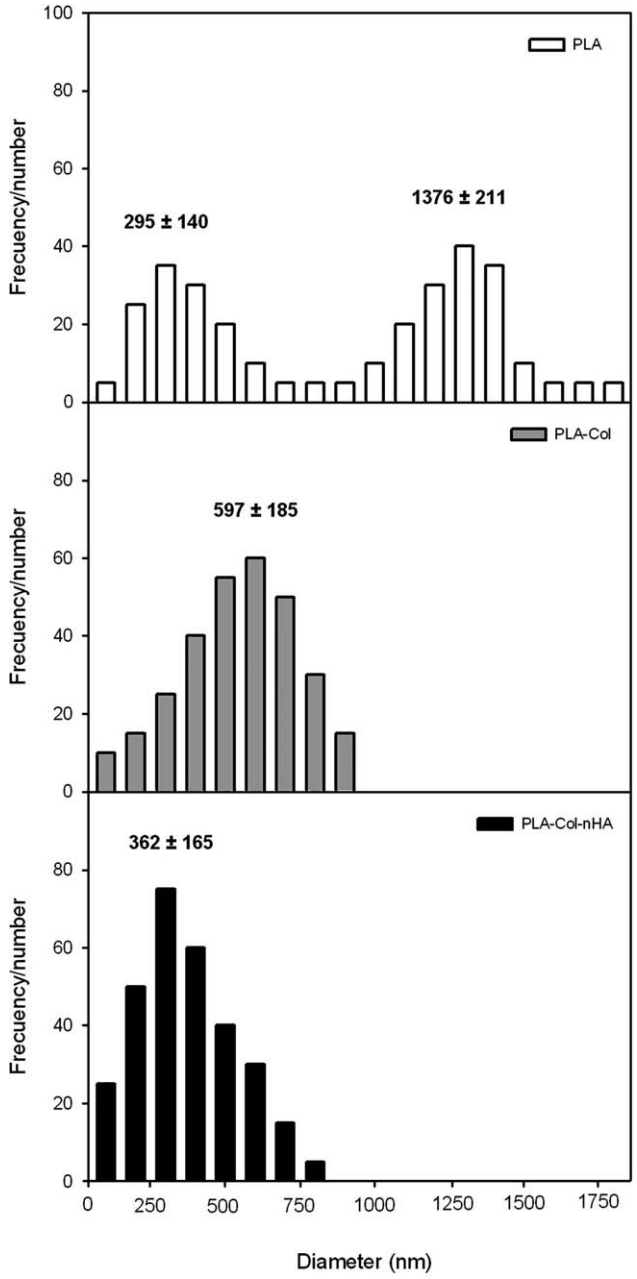

Figure 2 Typical size distributions of electrospun PLA-based fibers: (a) pure PLA, (b) PLA-Col, and (c) PLA-Col-nHA.

naturally grow elongated in the fiber axis direction. In the present work, the nHA crystals were introduced first into pure collagen and then electrospun [see Fig. 4(a)], later into the PLA-collagen solution [Fig. 4(b)], and then again electrospun to form the so-called tricomponent fibers mat. A good dispersion of the nHA crystals within the collagen fibers is seen by TEM observation where individual crystals of nHA are clearly discerned. A similar TEM image obtained in the tricomponent system is observed, which again proves that the nHA particles are embedded in the fibers but with lower dispersion and homogeneity due to probably lower compatibility with the polyester phase. A similar morphological irregular dispersion has been previously found for carbon nanotubes within poly(ethylene oxide) electrospun fibers.[40] The tricomponent system was water resistant as opposed to the neat collagen electrospun nanofibers, which are known to easily disperse in water.[30] In any case, it is expected that the nHA should preferentially align in the collagen rich part of the tricomponent fibers and that the collagen will be water resistant given the comparatively lower water-induced plasticization of the PLA. Both images in Figure 4 show that single nHA crystals inside electrospun fibers have a rodlike morphology and with lengths and widths between 40 and 130 nm and between 20 and 50 nm, respectively.

Regarding nHA orientation within the fiber axis, some electrospinning works have already proven that the extensional forces exerted by the electrospinning apparatus tend to mechanically align the embedded nanoparticles in the fibers as Figure 4 suggests.[40,41] This results in orientation of the nHA crystals approximately parallel to the electrospun fiber axis, effect that resembles the natural bonding patterns found in natural bone.[42]

Fibers composition

To characterize the molecular composition of the developed electrospun PLA-based materials, ATR-FTIR spectroscopy was applied (see Fig. 5). The data of the multicomponent fibers, that is to say, the so-called bicomponent and tricomponent fibers, are compared to the pure components and also with the sterilized sample in Figure 5(a). The FTIR spectrum of the pure electrospun PLA fibers shows a major band at about 1750 cm^{-1}, which is assigned to C=O stretching.[43] Second major bands for PLA were seen in the range 1050–1250 cm^{-1}, which are thought to arise from C—O and C—O—C stretching vibrations.[41] There are also three bands in the range 1300–1500 cm^{-1} that are assigned to symmetric and asymmetric deformational vibrations of C—H in the CH_3 groups.[43,44] Previously prepared pure electrospun collagen nanofibers,[30] also presented three main band envelops, which are respectively, assigned to the C=O stretching of the amide I at 1600–1700 cm^{-1}, C—N stretching, and N—H bending combination of the amide II at 1500–1600 cm^{-1}, and C—N stretching, N—H bending, and C—C stretching of the amide III at 1200–1300 cm^{-1}.[45] These amide band regions of the collagen spectrum are directly related to polypeptide conformations.[45] For the nHA powder, main absorptions were seen at $\sim$ 960 cm^{-1} associated to the PO_4^{-3} stretch υ_1 and from 1000 to 1100 cm^{-1} to PO_4^{-3} bend $\upsilon 3$.[46]

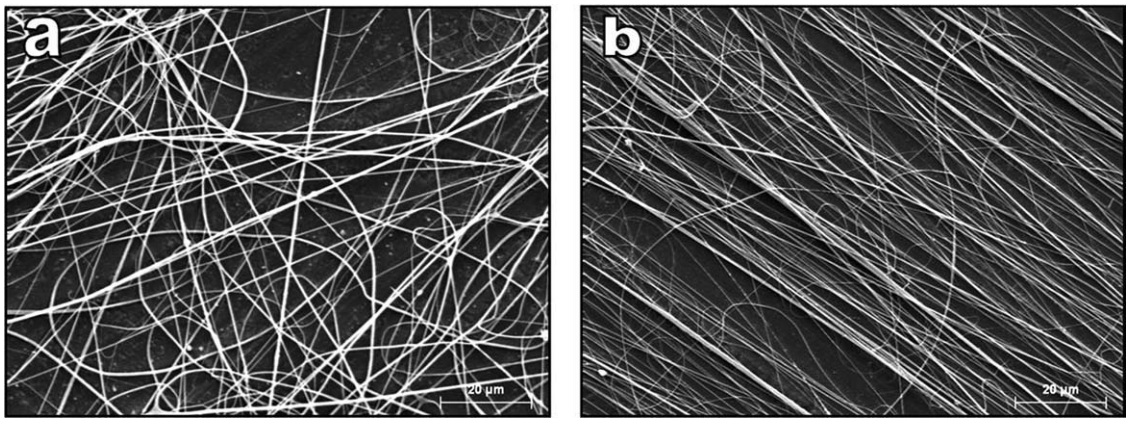

Figure 3 SEM images taking on the PLA-collagen-nHA fiber mats: (a) random fiber mat deposited on static collector; (b) aligned fiber mat deposited onto a rotating mandrel. The scale marker is 20 μm.

The presence of the added bioactive components to PLA can be verified from the ATR-FTIR spectra. Along with the three amide bands derived from collagen, which can be observed in the bicomponent mat, the tricomponent mat additionally show the phosphate bands, characterizing the presence of the naturally occurring mineral phase in the fiber structure. Figure 5(b) shows a spectral zoom highlighting the presence of two new bands centered at 1655 and 1550 cm^{-1}, attributed to collagen amides I and II, respectively. Figure 5(c) highlights the major spectral changes produced in the tricomponent fiber spectrum by the addition of the bioactive mineral. Furthermore, FTIR analysis has been proven to be a reliable tool to determine the effect of sterilization, in particular, γ-irradiation, on biomedical materials.[47] Spectral comparisons, before and after sterilization, did not yield significant differences between the two top spectra of Figure 5(a), suggesting the absence of detectable chemical alterations due to sterilization.

Thermal properties

The effect of the presence of the different components on the thermal stability of the tricomponent fiber mat was studied by means of DSC and TGA techniques. First, DSC was applied to evaluate the impact of adding the bioactives collagen and nHA, and also of the sterilization process, on the glass transition temperature (T_g), cold crystallization temperature (T_{cc}), melting temperature (T_f), and crystallinity index ($\%X_c$) of the materials (see Table I). Figure 6 shows the DSC thermograms taken in, from top to bottom, nHA, electrospun collagen, PLA, bicomponent system, tricomponent system, and sterilized tricomponent fibers. Electrospun collagen is known to denature around 67°C,[30] whereas the T_g, T_{cc}, and T_f of electrospun PLA occur at 62.7, 93.2, and 150.7°C, respectively, in good agreement with previous thermal characterization work.[48] Adding collagen altered the PLA thermal properties, and it was seen that the electrospun bicomponent fibers showed lower T_g, T_{cc}, and T_m,

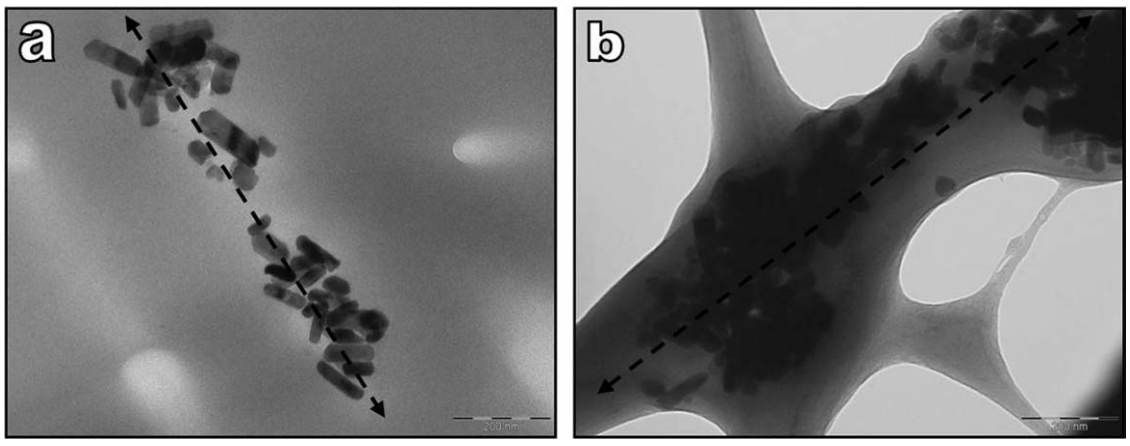

Figure 4 TEM images of (a) the collagen-nHA system and (b) of the PLA-collagen-nHA system. Arrows indicate the direction of the fiber axis and the scale marker is 200 nm.

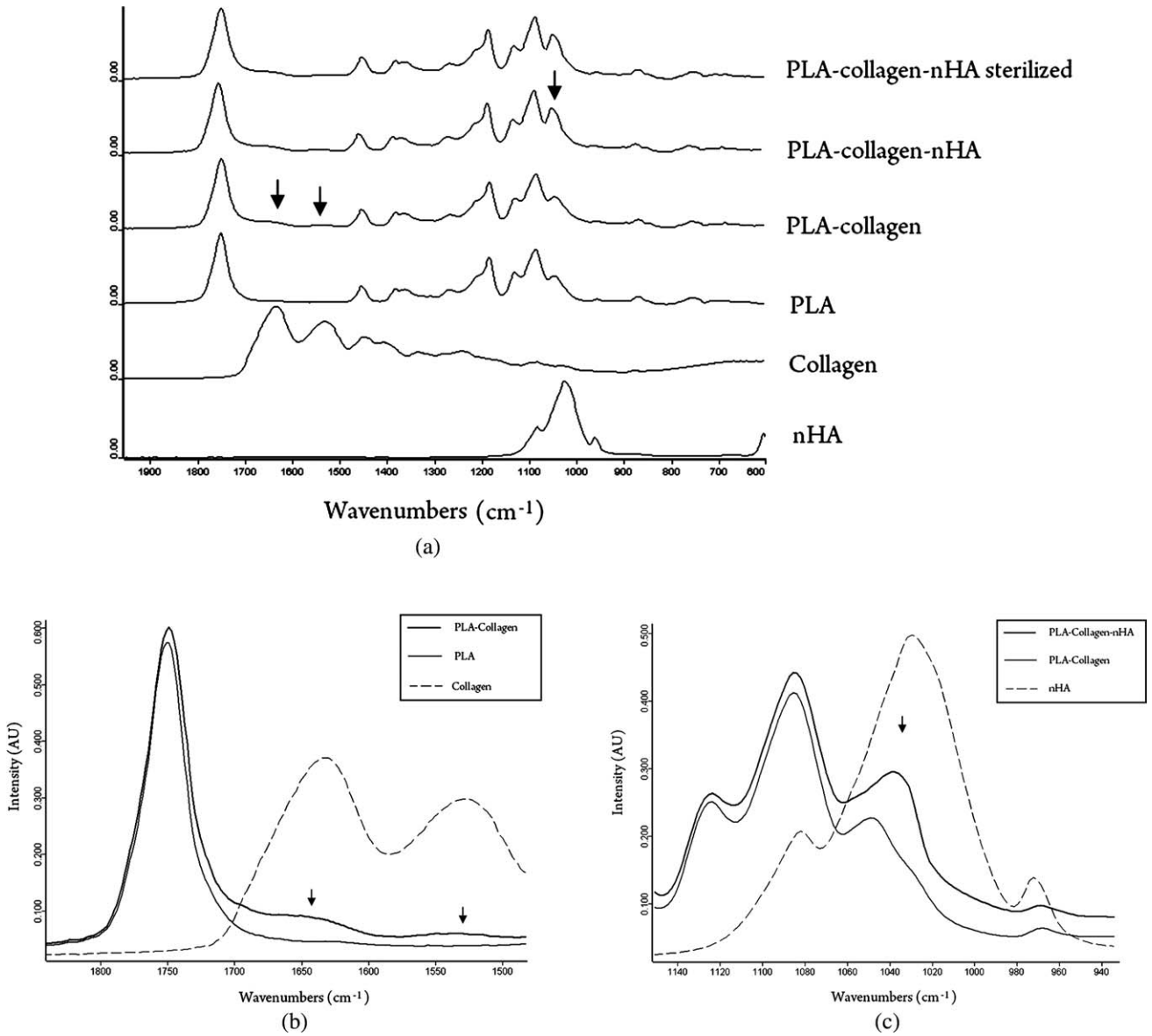

Figure 5 ATR-FTIR spectra of (a) full spectra of all components; (b) zoom in the range 1450–1840 cm^{-1}; (c) zoom in the range 930–1150 cm^{-1}. Arrows indicate major changes in the biomaterials.

that is, 58.1, 87.3, and 148.4°C, respectively. This effect can be attributed to collagen molecules plasticizing the material and altering the crystallization behavior of this by incorporation in between polylactide chains after electrospinning. For the tricomponent fibers, similar thermal behavior was observed, but the biomineral loading increased to some extent the thermal values up to 59.5, 88.7, and 149.1°C, respectively. Finally, the sterilized tricomponent fibers exhibited similar thermal properties than the nonsterilized fibers, suggesting again that γ-irradiation does not bring any additional

TABLE I
Glass Transition Temperature (T_g), Cold Crystallization Temperature (T_{cc}), Melting Temperature (T_m), and Crystallinity Index (%X_c) of PLA-Based Fibers as Four Determined from DSC Endotherms

Sample	T_g (°C)	T_{cc} (°C)	T_f (°C)	X_c (%)
PLA	62.7 ± 1.3	93.2 ± 1.8	150.7 ± 1.9	6.6 ± 0.3
PLA-Col	58.1 ± 0.9	87.3 ± 1.4	148.4 ± 1.7	2.4 ± 0.1
PLA-Col-nHA	59.5 ± 1.1	88.7 ± 1.3	149.1 ± 1.8	2.9 ± 0.2
PLA-Col-nHA sterilized	59.4 ± 0.8	88.4 ± 1.5	148.9 ± 1.6	2.7 ± 0.2

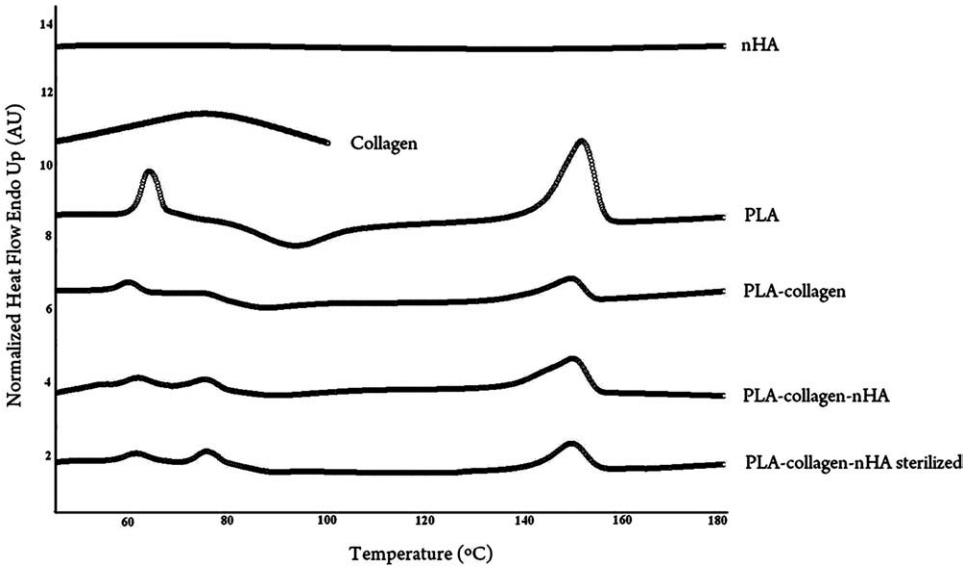

Figure 6 DSC melting endotherms of nHA powder, electrospun collagen, PLA, bicomponent, tricomponent, and sterilized tricomponent fibers.

impact on the thermal properties of the PLA-based fibers. In accordance with the above, the PLA crystallinity was decreased in the blends, suggesting that the bioactives in the fibers hindered the formation of crystallinity in the material.

TGA experiments were run in parallel to determine the thermal stability of the PLA-based fiber mats. Figure 7 presents the thermal degradation profiles of nHA, electrospun collagen, PLA, bi-, and tricomponent fiber mats, and Table II gathers the mass loss obtained from the plots. As recently showed in other thermal study carried out for electrospun polymers,[49] the mass loss occurred in three stages: the first one refers to the loss of moisture, solvent, and structural water (25–200°C); the second to the thermal degradation of the network structure (200–400°C); and the third stage (400–800°C) to the carbonization of polymeric materials. Adding collagen produced a decrease in the PLA thermal properties, because the maximum of the first derivative was reduced from 352.4 to 309.5°C. Recent literature has confirmed that the thermal degradation of collagen is mainly produced around 300°C,[50] while PLA lasts up to 400°C.[51] With regard to the tricomponent fiber mat, it can be seen that the apatite mineral is stable up to ~ 800°C (98.3%), in agreement with previous literature.[52] As a result of this, the TGA of the tricomponent fibers showed a similar thermal profile than that of the bicomponent fibers but with a residue of about 9.7 wt % corresponding to the remaining mineral mass at 800°C. It is also noticeable to observe that the biomineral presence in the tricomponent fibers slightly enhanced the thermal stability of the bicomponent fibers as the peak increased to 317.6°C.

Cell behavior

A cell growth test using osteoblastlike human cells was conducted to ascertain the osteoconductivity of the different PLA-based materials. Cell numbers, as determined from the Alamar Blue assay, increased with time, as illustrated in Figure 8, and reached a plateau after 11–14 days. The comparison, in terms of biocompatibility, of a PLA film, PLA fiber mat, bicomponent fiber mat, tricomponent fiber mat, and aligned tricomponent fiber mat showed very dissimilar performance regarding cell viability. It is seen that the biggest increase in the proliferation cell rate is observed when the PLA morphology is changed from a flat film to electrospun submicrofibers (~ 18% higher at day 4 and 43% at day 14). As previously discussed, the electrospun nanostructure could result to be similar to that found in natural bone and thus could be identified as "bone" by the attached cells. Regarding this, although native human bones are also known to compromise collagen fibrils of ~ 50 nm and are very uniform in size,[53] some fibrils can be accepted to have fiber diameters as broad as 500 nm.[54] Introducing collagen, a natural and well-recognized osteoconductive biopolymer,[30] additionally increased the cell population during the initial days, that is, cell growth was 11% higher at day 4. A similar effect in cell proliferation was observed when nHA was added to the bicomponent fiber mat, which resulted in ~ 12% higher viability at day 4. Furthermore, similar *in vitro* experiments were performed in the tricomponent fiber mat after sterilization with γ-irradiation, and no relevant differences were observed. Finally, when the rotating frame cylinder was used as the

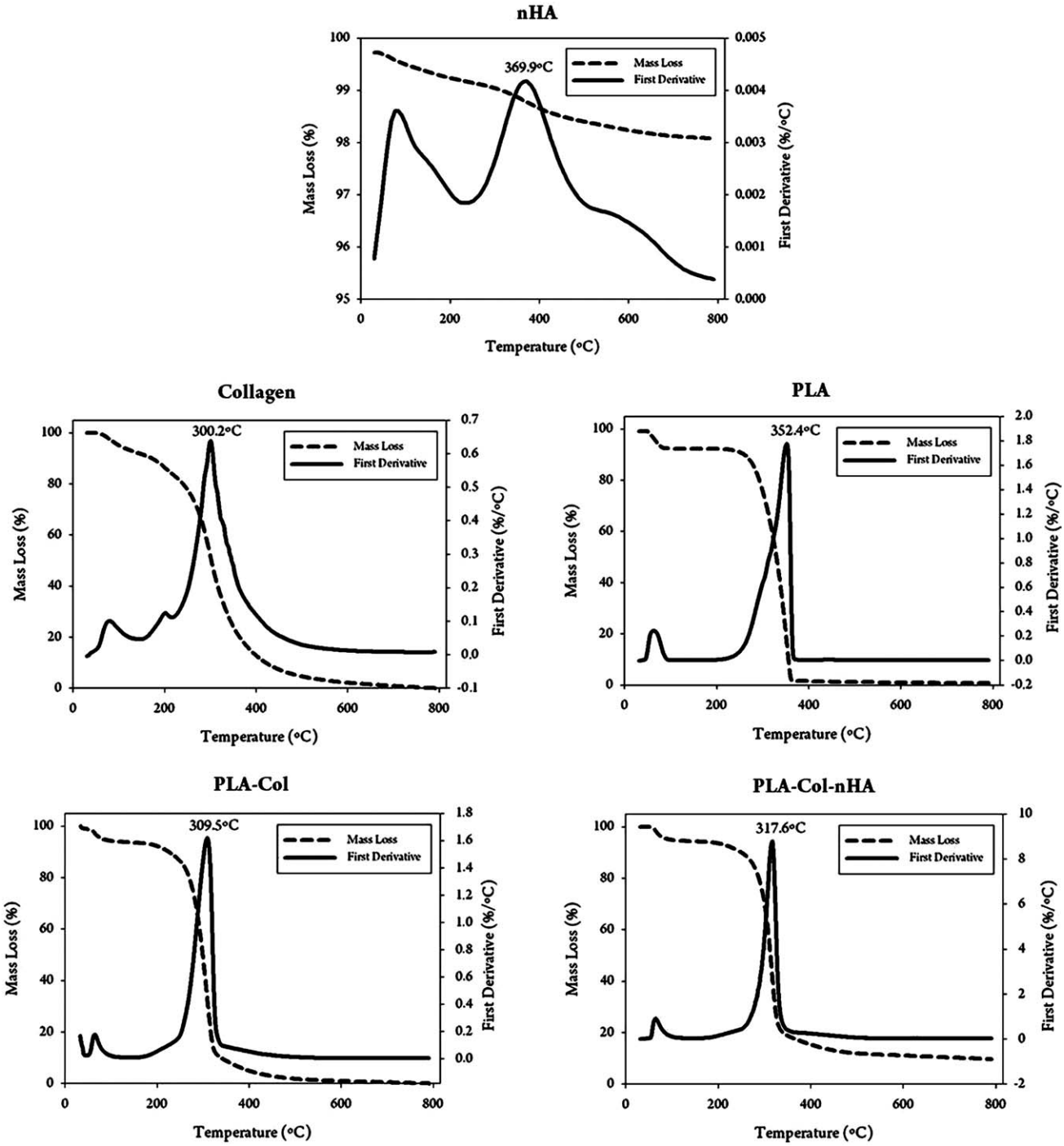

Figure 7 TGA mass loss and first derivative curves of collagen and PLA-based fibers.

fiber collector, the highest cell viability was obtained for the tricomponent mat, which resulted in an increase of 14% at day 4. At the end of the experiment, that is, days 10–14, all electrospun interfaces presented very similar cell growth values, which indicate that either the cells can be equally stabilized with time in all fiber mats or the cell assay reached its maximum measurable value.

Figure 9 shows SEM images in which the progressive harvested cells adhered onto the fiber mat increases over time on the sterilized tricomponent fiber mat. Although this image well illustrates cell evolution on the mat, it did not provide accurate information about living cells attachment or the interaction between cells and the electrospun interfaces. For a more precise morphology assessment, optical microscopy using a fluorescent dye and a FITC filter was used. Figure 10 shows that the MG-63 osteoblasts adhered and spread on the surface of the mat. Comparison of both images (bright field and

TABLE II
Collagen and PLA-Based Fiber Mat Weight Losses (%) as Determined by TGA

Sample	% Weight loss		
	25–200°C	200–400°C	400–800°C
nHA	0.6 ± 0.1	0.8 ± 0.2	0.3 ± 0.1
Collagen	13.7 ± 1.1	78.2 ± 2.8	8.1 ± 1.3
PLA	6.9 ± 0.5	92.6 ± 4.4	0.5 ± 0.2
PLA-Col	8.1 ± 0.3	86.7 ± 2.9	5.2 ± 0.6
PLA-Col-nHA	7.8 ± 0.7	77.8 ± 3.6	4.7 ± 0.8

fluorescence light) showed that cells, in green, presented a fibroblastlike structure and were developed on top of the fiber architecture. Although most cells were seen to interact with upper fiber layer, some of them also seemed to be integrated in lower levels or in suspension. Therefore, the tricomponent fibrous scaffold, PLA-collagen-nHA, seem to present enough porosity and high-surface area-to-volume ratios to provide a favorable environment for osteoblast attachment and proliferation.

CONCLUDING REMARKS

In tissue-engineering applications, it is generally recognized that the first and essential requiring step is to produce a nanostructured surface morphology, which is thought to best mimic native tissues. Because of the extremely high-surface-to-volume ratio as well as the good uniformity, electrospun fibers are being currently considered as feasible interfaces or coatings of implants to generate osteoconductive surfaces. In the present work, a PLA-based electrospun nanostructured fiber mat formulations were optimized for the purpose of the application. It was first proven that the ultrathin fiberlike fabrication of PLA produced a relevant increase in biocompatibility compared to sheets or bulk fabrications of PLA.

In spite of PLA being mechanical robust, inexpensive, noncytotoxic, and a resorbable polymer with desired degradation rates, this biomaterial is not considered to have an adequate chemical recognition to regulate different cell behaviors such as cell proliferation. Thus, blending PLA with more bioactive components, such as collagen (bicomponent fibers) and collagen and nHA (tricomponent fibers), was carried out and found to considerably enhance osteoblastlike cell proliferation. These bioactive coatings are thought to comprise effective affinity for regulating specific cell functions. It was also found that uniaxial alignment of the cited fibers by using a high-speed-rotating collector resulted in further increase in cell-seeding capacity.

Finally, a requiring procedure in implants is the sterilization of the product before undertaking surgery. This necessary process is often disregarded by biomaterials scientists in the evaluation of their developments. This work presents for the first time the evaluation of the impact of a γ-irradiation process on the morphology, stability, and biocompatibility of PLA-based fiber mats. From the results, the irradiated fibers did not show any noticeable impact in the cited properties, hence clearing up any

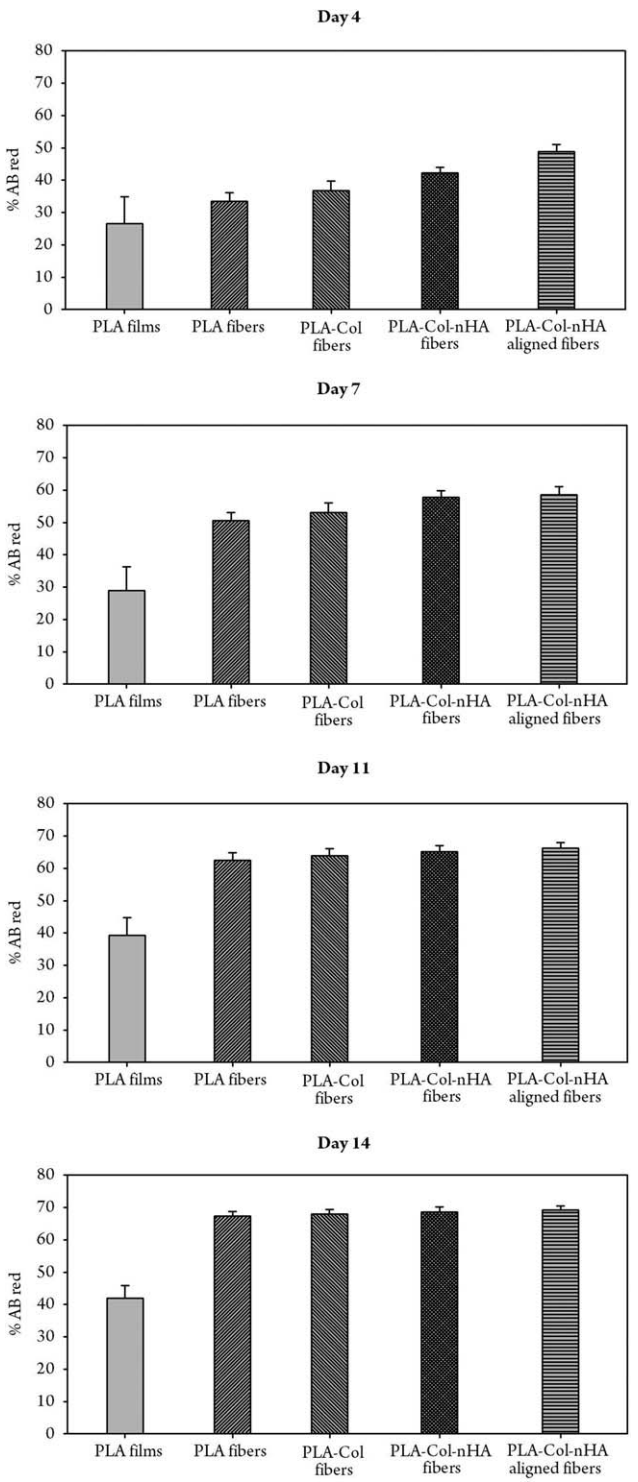

Figure 8 Cell viability tests of the various systems as a function of time.

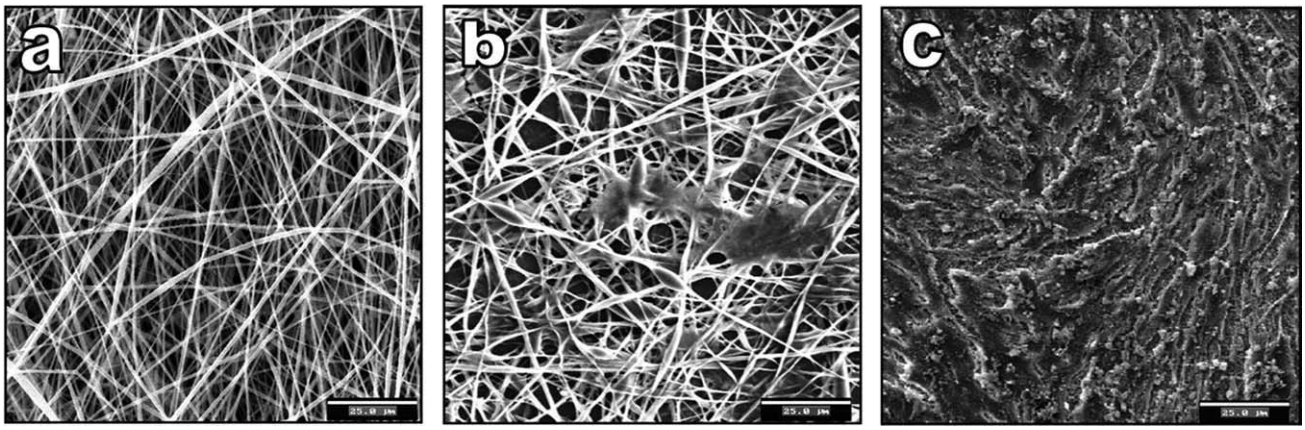

Figure 9 SEM images of the sterilized tricomponent system during cell grow tests: (a) beginning of test; (b) after 4 days; (c) after 14 days. The scale marker is 25 μm.

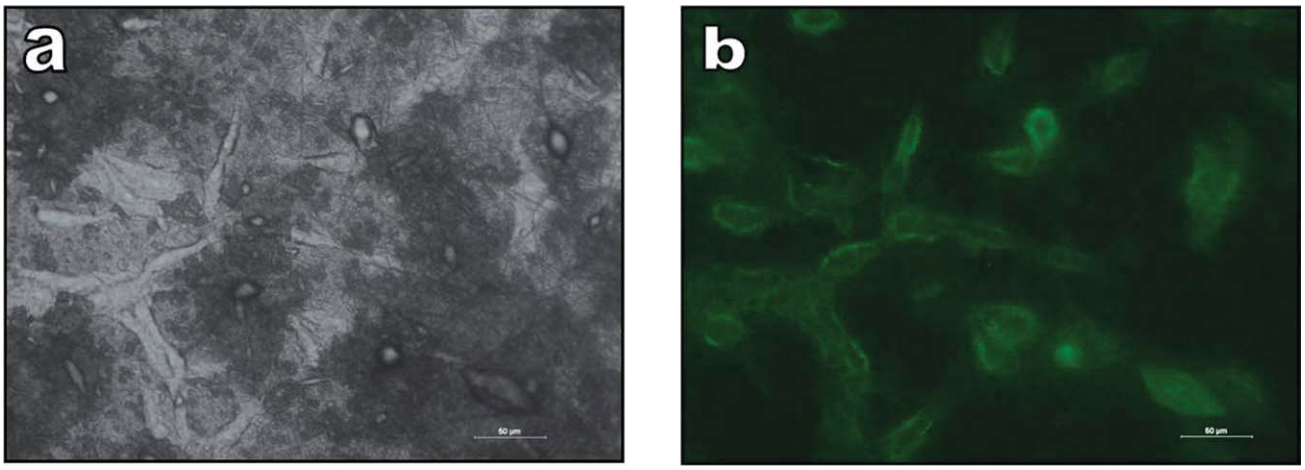

Figure 10 Typical optical micrographs of the cell growth of sterilized electrospun tricomponent fiber mat under (a) bright field light; (b) fluorescence with FITC filter. The scale marker is 50 μm. [Color figure can be viewed in the online issue, which is available at wileyonlinelibrary.com.]

obstacles as to the potential application of these materials in biomedical applications.

The authors thank Dr. Michaelis Vardavoulias and Dr. Rosanna Gonzalez-McQuire from pyrogenesis for the supplied materials within the context of the NEWBONE project.

References

1. Gupta, A. P.; Kumar, V. Eur Polym J 2007, 43, 4053.
2. Navarro, M.; Ginebra, M. P.; Planell, J. A.; Barrias, C. C.; Barbosa, M. A. Acta Biomater 2005, 1, 411.
3. Biondi, M.; Ungaro, F.; Quaglia, F.; Netti, P. A. Adv Drug Deliv Rev 2008, 60, 229.
4. Park, A.; Wu, B.; Griffith, L. G. J Biomater Sci Polym Ed 1998, 9, 89.
5. Yang, X.; Yuan, M.; Li, W.; Zhang, G. J Appl Polym Sci 2004, 94, 1670.
6. Kothapalli, C. R.; Shaw, M. T.; Wei, M. Acta Biomater 2005, 1, 653.
7. Liao, S. S.; Cui, F. Z.; Zhang, W.; Feng, Q. L. J Biomed Mater Res B 2004, 69, 158.
8. Wahl, D. A.; Czernuszka, J. T. Eur Cells Mater 2006, 11, 43.
9. Wong, W. H.; Mooney, D. J. In Synthetic Biodegradable Polymer Scaffolds; Atala, A., Mooney, D., Vacanti, J. P., Langer, R., Eds.; Birhauser: Boston, MA, 1997; p 50.
10. Mooney, D. J.; Langer, R. S. In The Biomaterials Handbook; CRC Press: Boca Raton, FL, 1995; p 1609.
11. Boland, E. D.; Wnek, G. E.; Simpson, D. G.; Pawlowski, K. J.; Bowlin, G. L. J Macromol Sci Part A: Pure Appl Chem 2001, 38, 1231.
12. Langer, R.; Vacanti, J. P. Science 1993, 260, 920.
13. Olsen, B. R. In Principles of Tissue Engineering; Lanza, R., Langer, R., Chick, W., Eds.; Academic Press: San Diego, CA, 1997; p 47.
14. Venugopal, J.; Low, S.; Choon, A. T.; Ramakrishna, S. J Biomed Mater Res B 2007, 84, 34.
15. Lannutti, J.; Reneker, D.; Ma, T.; Tomasko, D.; Farson, D. Mater Sci Eng C 2007, 27, 504.
16. Albrektsson, T.; Johansson, C. Eur Spine J 2001, 10, S96.
17. Wen, X. T.; Fan, H. S.; Tan, Y. F.; Cao, H. D.; Li, H.; Gai, B.; Zhang, X. D. Key Eng Mater 2005, 288–289, 139.
18. Inai, R.; Kotaki, M.; Ramakrishna, S. Nanotechnology 2005, 16, 208.
19. Chiu, J. B., Liu, C.; Hsiao, B. S.; Chu, B.; Hadjiargyrou, M. J Biomed Mater Res A 2007, 83, 1117.
20. Thomas, V.; Dean, D. R.; Vohra, Y. K. Curr Nanosci 2006, 2, 155.

21. Kim, H.-W.; Lee, H.-H.; Knowles, J. C. J Biomed Mater Res A 2006, 79, 643.
22. Kim, H.-W.; Lee, H.-H.; Chun, G.-S. J Biomed Mater Res A 2008, 85, 651.
23. Li, D.; Xia, Y. Adv Mater 2004, 16, 1151.
24. Xu, C. Y.; Inai, R.; Kotaki, M.; Ramakrishna, S. Biomaterials 2004, 25, 877.
25. Martins-Green, M. In Principles of Tissue Engineering; Lanza, R., Langer, R., Chick, W., Eds.; R. G. Landes Company: Georgetown, TX, 1997; p 23.
26. Zhu X, Cui W, Li X, Jin Y. Biomacromolecules 2008, 9, 1795.
27. Matthews, J. A.; Simpson, D. G.; Wnek, G. E.; Bowlin, G. L. Biomacromolecules 2002, 3, 232.
28. Friess, W. Eur J Pharm Biopharm 1998, 45, 113.
29. Clough, R. L. Nucl Instrum Methods B 2001, 185, 8.
30. Torres-Giner, S.; Gimeno-Alcañiz, J. V.; Ocio, M. J.; Lagaron, J. M. Appl Mater Interfaces 2009, 1, 218.
31. Torres-Giner, S.; Gimenez, E.; Lagaron, J. M. Food Hydroc 2008, 22, 601.
32. Liu, X.; Dever, M.; Fair, N.; Benson, R. S. J. Environ Polym Degrad 1997, 5, 225.
33. Peesan, M.; Rujiravanit, R.; Supaphol, P. J Biomater Sci Polymer Ed 2006, 17, 547.
34. Koombhongse, S.; Liu, W. X.; Reneker, D. H. J Polym Sci B 2001, 39, 2598.
35. Torres-Giner, S.; Ocio, M. J.; Lagaron, J. M. Carbohydr Polym 2009, 77, 261.
36. Casper, C. L.; Stephens, J. S.; Tassi, N. G.; Chase, D. B.; Rabolt, J. F. Macromolecules 2004, 37, 573.
37. Torres-Giner, S.; Ocio, M. J.; Lagaron, J. M. Eng Life Sci 2008, 8, 303.
38. Weiner, S.; Price, P. A. Calc Tissue Int 1986, 39, 365.
39. Weiner, S.; Traub, W. FEBS Lett 1986, 206, 262.
40. Dror, Y.; Salalha, W.; Khalfin, R. L.; Cohen, Y.; Yarin, A. L.; Zussman, E. Langmuir 2003, 19, 7012.
41. Salalha, W.; Dror, Y.; Khalfin, R. L.; Cohen, Y.; Yarin, A. L.; Zussman, E. Langmuir 2004, 20, 9852.
42. Robinson, R. A.; Watson, M. L. Anat Rec 2005, 114, 383.
43. Paragkumar, N. T.; Edith, D.; Jean-Luc, S. Appl Surf Sci 2006, 253, 2758.
44. Braun, B.; Dorgan, J. R.; Dec, S. F. Macromolecules 2006, 39, 9302.
45. Camacho, N. P.; West, P.; Torzilli, P. A.; Mendelsohn, R. Biopolymers 2001, 62, 1.
46. Panda, R. N.; Hsieh, M. F.; Chung, R. J.; Chin, T. S. J Phys Chem Sol 2003, 64, 193.
47. White, J. M.; Goodis, H. E.; Marshall, S. J.; Marshall, G. W. J Dent Res 1994, 73, 1560.
48. Zong, X.; Kim, K.; Fang, D.; Ran, S.; Hsiao, B. S.; Chu, B. Polymer 2002, 43, 4403.
49. Torres-Giner, S.; Lagaron, J. M. J Appl Polym Sci 2010, 118, 778.
50. Horn, M. M.; Martins, V. C. A.; Plepis, A. M. G. Carbohydr Polym 2009, 77, 239.
51. Badia, J. D.; Moriana, R.; Santonja-Blasco, L.; Ribes-Greus, A. Macromol Symp 2008, 272, 93.
52. Li, Y.; Tjandra, W.; Tam, C. Mater Res Bull 2008, 43, 2318.
53. Nimni, M.; Harkness, R. In Molecular Structures and Functions of Collagen, Vol.I: Biochemistry; CRC Press: Boca Raton, FL, 1988; p 3.
54. Elsdale, T.; Bard, J. J Cell Biol 1972, 54, 626.